Journal of Fluorine Chemistry 178 (2015) 131–135

Contents lists available at ScienceDirect

Journal of Fluorine Chemistry

journal homepage: www.elsevier.com/locate/fluor

# Synthesis, crystal structure, and properties of pentadecafluorotetraantimonate(III) $CsRb_2Sb_4F_{15}$

L.A. Zemnukhova, A.A. Udovenko, N.V. Makarenko *, G.A. Fedorishcheva, M.M. Polyantsev, V.Ya. Kavun

*Institute of Chemistry, FEBRAS, 159, Pr. 100-letiya Vladivostoka, Vladivostok 690022, Russia*

ARTICLE INFO

*Article history:*
Received 1 June 2015
Received in revised form 6 July 2015
Accepted 9 July 2015
Available online 17 July 2015

*Keywords:*
Synthesis
Structure
Cesium–rubidium
pentadecafluorotetraantimonate(III)
Ionic mobility
Ionic conductivity
$^{19}F$ NMR spectra

ABSTRACT

A new compound $CsRb_2Sb_4F_{15}$ (**I**) has been synthesized, and its crystal structure (monoclinic syngony: $a$ = 7.9863(3), $b$ = 28.594(1), $c$ = 8.0319(3) Å, $\beta$ = 116.60(1), space group $P2_1/c$) has been determined. The structure of **I** is composed of complex $[Sb_2F_7]^-$ and $[SbF_4]^-$ anions and $Cs^+$ and $Rb^+$ cations, which link structural units into a framework through ionic bonds. The isostructural character of the compounds $CsRb_2Sb_4F_{15}$ (**I**) and $Cs_3Sb_4F_{15}$ (**II**) has been established. It has been demonstrated that fluorine ions diffusion is a predominant type of ionic motions in the fluoride sublattice of the compound **I** above 420 K. The comparison of ionic conductivities in $K_3Sb_4F_{15}$, $Cs_3Sb_4F_{15}$, and $CsRb_2Sb_4F_{15}$ complexes has been performed. The factors determining the value of ionic conductivity in these compounds have been discussed.



## 1. Introduction

In aqueous solutions, antimony trifluoride interacts with fluorides of alkali metals and ammonium with formation of crystalline complex antimonates(III) with different F:Sb ratios in dependence on the molar ratio of the initial components. A substantial effect on the composition, structure, and properties of such compounds is provided by the nature of the outer-sphere cation. The structure and physical–chemical properties of many complex penta-, tetra-, and heptafluoroantimonates(III) as with homogeneous as with mixed monovalent cations have been investigated rather thoroughly [1–11]. Many compounds in these series are characterized by the presence of phase transitions with formation of modifications, in which the diffusion of fluorine (ammonium) ions causing high ionic conductivity is a dominating type of ionic motions [3,4,10–12]. The compounds belonging to the group of pentadecafluoroantimonates(III), in which the ratio F:Sb = 3.75, have been studied insufficiently. The available literature contains the reports on the solid-phase synthesis of complexes $M_3Sb_4F_{15}$ (M = K, Rb, Cs) [3] and the classic synthesis of compounds of such compositions with potassium [10], cesium, and ammonium [13–15] cations from aqueous solutions. Each of the known structures of $M_3Sb_4F_{15}$ (M = Cs, $NH_4$) contains four crystallograhically independent antimony atoms, whereas the compounds themselves are not isostructural to each other [15]. The formation of superionic phases having the conductivity around $10^{-3}$–$10^{-2}$ S/cm ($T > 440$ K) was established at studies of the character of ionic motions and phase transitions in the compounds $(NH_4)_3Sb_4F_{15}$, $Cs_3Sb_4F_{15}$, and $K_3Sb_4F_{15}$ [10,14]. However, the available literature does not contain the data on compounds of this class with heteroatomic cations of the composition $M_{3-x}M_x'Sb_4F_{15}$ ($M \neq M'$ – the alkali cation). It is well-known [7,16] that the structure and properties of fluorocomplexes with mixed and homogeneous outer-sphere cations could differ, while for many complexes with mixed cations dynamic processes in anionic and cationic sublattices could be observed at lower temperatures than for compounds with homogeneous outer-sphere cations. Upon the isomorphic substitution of a part of cesium ions by rubidium ions in the superionic conductor $Cs_3Sb_4F_{15}$, we obtained the complex $CsRb_2Sb_4F_{15}$, whose structure and some properties are under examination in the present paper. Here, the structural data for the complex fluoroantimonate(III) with the mixed cationic sublattice are presented for the first time.

* Corresponding author. Tel.: +7 423 2215275x323; fax: +7 423 2311889.
*E-mail address:* makarenko@ich.dvo.ru (N.V. Makarenko).

http://dx.doi.org/10.1016/j.jfluchem.2015.07.014
0022-1139/

## 2. Results and discussion

### 2.1. IR spectroscopy

Fig. 1 shows IR absorption spectra of the complexes $CsRb_2Sb_4F_{15}$ (**I**) and $Cs_3Sb_4F_{15}$ (**II**), in which one can observe characteristic bands of Sb–F bonds [17].

### 2.2. Crystal structure of $CsRb_2Sb_4F_{15}$

The crystal structure of the compound **I** is an isle-like (Fig. 2). Its main structural elements include dimeric $[Sb_2F_7]^-$ anions (Sb(1) and Sb(2) atoms), isolated $[SbF_4]^-$ anions (Sb(3) and Sb(4) atoms), and $Cs^+$ and $Rb^+$ cations linked by ionic bonds into a three-dimensional framework. The structure contains four crystallographically independent antimony atoms, whose coordination polyhedra are trigonal $SbF_4E$ bipyramids: two of these bipyramids are linked to the $[Sb_2F_7]^-$ dimer. Geometric parameters of polyhedra of the compound **I** (see Table in supporting information) are similar to those described in [15] for the complex **II**. 8- and 9-vertex structures are the coordination polyhedra (CP) of the Rb1 and Rb2 atoms with Rb-F distances 2.795–3.230 Å, whereas a 8-vertex structure is the CP of the Cs atom with Cs-F distances 3.091–3.367 Å.

Similar surrounding of outer-sphere cations is present in the structure of $Cs_3Sb_4F_{15}$ as well (Cs1: 2.926–3.336; Cs2: 2.986–3.224; Cs3: 3.087–3.436 Å). One should mention that the isomorphic substitution of Cs atoms by Rb atoms took place in positions where the coordination spheres of Cs atoms were significantly smaller.

### 2.3. Ion mobility in CsRb2Sb4F15, NMR data

$^{19}F$ NMR spectra of the compound $CsRb_2Sb_4F_{15}$ at different temperatures are shown in Fig. 3. At low temperatures, the form of

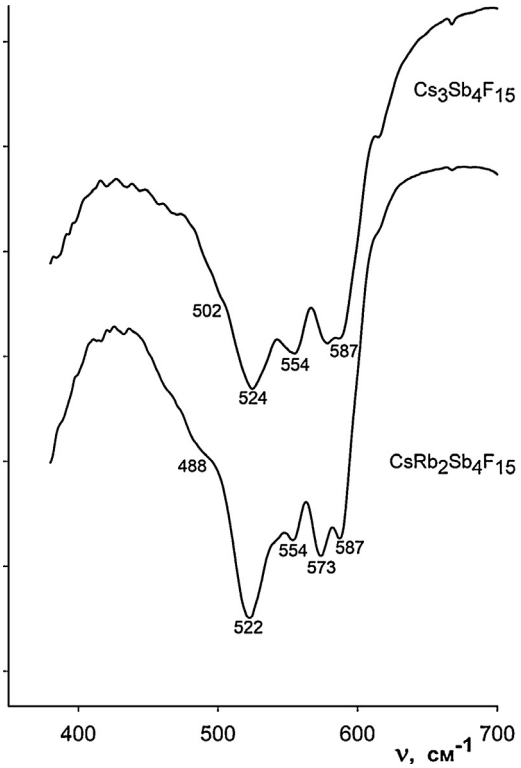


**Fig. 1.** IR absorption spectra of complexes **I** and **II**.

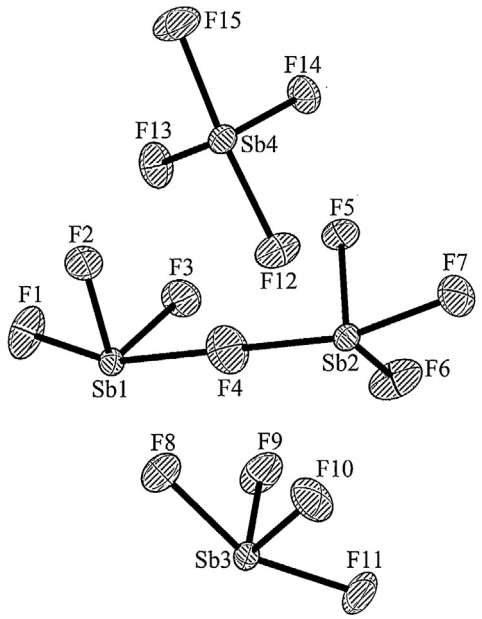


**Fig. 2.** Fragment of the crystal structure of **I**.

NMR spectra of this substance, just like that of $Cs_3Sb_4F_{15}$, is the result of structural nonequivalence of $F^-$ nuclei and anisotropy of the chemical shift. The observed spectra transformation upon temperature variation in the absence of phase transitions (the DSC curve does not contain endo-effects in the temperature range 300–470 K, the sample melting start point of the sample **I** is 477 K) is related to the transition of fluorine-containing groups of antimony(III) from one type of motion to another at the temperature increase from 150 up to 475 K. Taking into account the form of the NMR spectrum and its width around 150–200 K, one can state that no ionic motions with frequencies above $10^4$ Hz

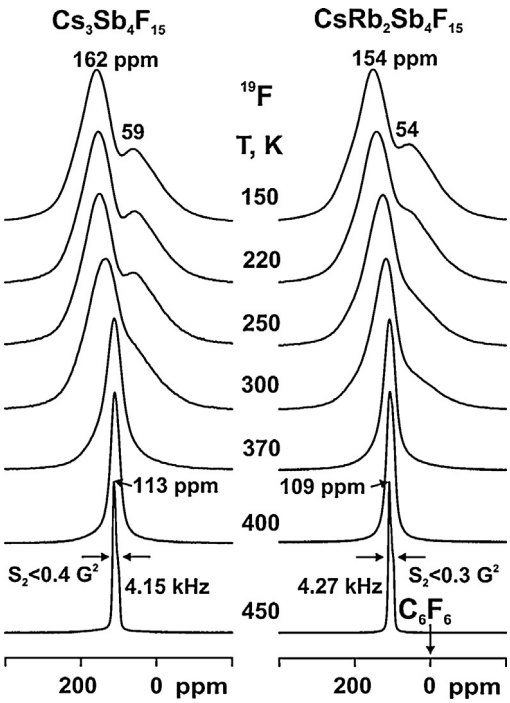


**Fig. 3.** Evolution of $^{19}F$ NMR spectrum shape versus temperature for the $Cs_3Sb_4F_{15}$ u $CsRb_2Sb_4F_{15}$ compounds.

are present in the fluorine sublattice below 200 K ('rigid lattice' in NMR terms [18]). In the case of the isostructural compound $Cs_3Sb_4F_{15}$, the rigid lattice is preserved until 270 K [10,19]. Heating above 200 K starts activation of local motions in the fluoride sublattice of **I**, which results in general spectrum narrowing and changes in its form (Fig. 3). For the compound **II**, the local mobility emerges at temperatures above 280 K. In the temperature range 300–400 K, the $^{19}F$ NMR spectrum of the compound $CsRb_2Sb_4F_{15}$ transforms into a relatively symmetric line with the chemical shift of ≈109 ppm, the width of 8 kHz, and the secondary moment lower than 4 $G^2$. Note that the absence of the narrow component characteristic for $^{19}F$ NMR spectra of many complex fluoroantimonates(III) [10,12,20–22] and indicating to the emergence of local mobility (diffusion) in the fluoride sublattice implies that the studied fluoride sublattice of the compound **I** comprises a dynamically heterogeneous system, in which all the resonating nuclei are characterized by the same correlation time. Similar situation is characteristic for the $^{19}F$ NMR spectra of the compound $Cs_3Sb_4F_{15}$ (Fig. 3) in the temperature range 290–380 K [19]. However, unlike $CsRb_2Sb_4F_{15}$, the former compounds are characterized by higher temperature range with the observed transformation of $^{19}F$ NMR spectra. Analysis of the parameters of the NMR spectrum of the compound $CsRb_2Sb_4F_{15}$ at 400 K allows assuming that at this temperature (as in case of the complex $Cs_3Sb_4F_{15}$ [19]) the main type of ionic motions consists in reorientations of antimony fluorine-containing groups (trigonal $SbF_4E$ bipyramids). Along with the temperature increase up to 420 K, one observes the transformation of $^{19}F$ NMR spectra of the compound **I** related to changes in their form: the relatively symmetric line narrows and transforms into the one whose shape, according to the computer simulation data (error not higher than 3.5%), is similar to a tent (see Fig. 4). (The fraction of the impurity signal with the chemical shift ≈106 ppm is ∼1.5% of total spectrum area.)

Similar transformation of the $^{19}F$ NMR spectrum takes place in the compound $Cs_3Sb_4F_{15}$ above 420 K. Such a line shape is characteristic for the spectrum of a polycrystalline sample, resonating nuclei of which have an axial chemical shift anisotropy (CSA) [18]. In this case, the parameters of the axial-symmetric tensor are: $\delta_\perp$ = 111, $\delta_\parallel$ = 94.5 and $\delta_{iso}$ = 105.5 ppm ($T$ = 470 K). A registration of the signal of this shape above 420 K in the presence of diffusion in the fluoride sublattice (the NMR second moment is less than 0.15 $G^2$) means that an averaging of the CSA of fluorine atoms does not take place. It is possible in the case when atoms (ions) move along the same positions in the lattice (anisotropic diffusion of fluorine atoms). One should mention that at diffusion of fluorine atoms similar spectra are observed, for instance, in tetrafluoroantimonates(III) of potassium–ammonium [23] and in the compounds $(NH_4)_6Li(Na)Zr_4F_{23}$ [24,25], $M_2ZrF_4$ (M = $NH_4$, Tl) [26] etc.

In conclusion, note that isostructurality and virtually identical character of transformation of $^{19}F$ NMR spectra of the compounds $CsRb_2Sb_4F_{15}$ and $Cs_3Sb_4F_{15}$ provide grounds to assume that in $CsRb_2Sb_4F_{15}$, just like in the complex $Cs_3Sb_4F_{15}$, which is a superionic conductor [10], one must observe high ionic conductivity above 420 K. Fig. 5 shows Arrhenius dependencies of ionic

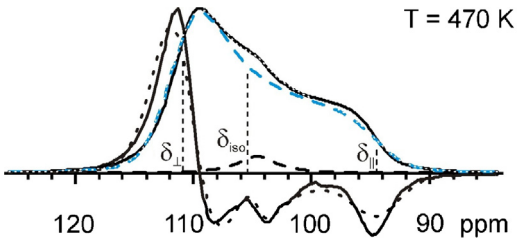


**Fig. 4.** Deconvolution of experimental $^{19}F$ NMR spectra for the $CsRb_2Sb_4F_{15}$ compound.

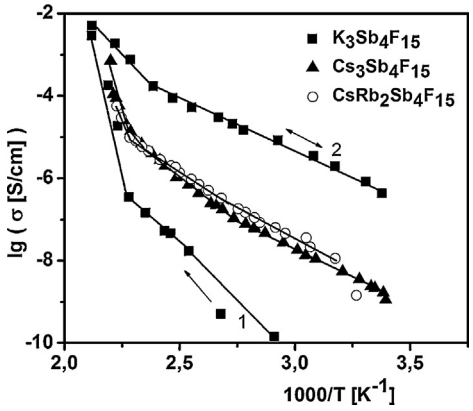


**Fig. 5.** Temperature dependences of conductivity for the compounds $CsRb_2Sb_4F_{15}$ and $M_3Sb_4F_{15}$ [10]; for $K_3Sb_4F_{15}$ arrows indicate the first heating (1) and subsequent heating–cooling cycles (2) for β-phase.

conductivity in the compounds $K_3Sb_4F_{15}$, $Cs_3Sb_4F_{15}$ [10], and $CsRb_2Sb_4F_{15}$ for comparison.

For the compounds **I** and **II**, a sharp knee on the temperature dependence $\lg(\sigma) = f(1/T)$ is in the temperature range 425–440 K is concerned with the transition of fluorine ions from local motions to diffusion. The value of the specific conductivity σ in the compound $CsRb_2Sb_4F_{15}$ at ∼450 K (maximal temperature of the experiment) is equal to $5.8 \times 10^{-5}$ S/cm that is an order of magnitude lower than that in $Cs_3Sb_4F_{15}$ at the same temperature ($6.9 \times 10^{-4}$ S/cm). Since the above compounds are isostructural, a possible reason of the decrease of the σ value in the compound with a heteroatomic cationic sublattice consists in the decrease of the number of cesium ions in its crystal lattice, since the presence of high-polarizability cations in the compound composition is known to be one of the factors responsible for high ionic conductivity [27–29]. In this case, cesium ions have higher polarizability than that of rubidium ions (2.400 and 1.437 $Å^3$, respectively [30]). Higher conductivity in the β-phase of potassium fluoroantimonate(III) in comparison to that of $Cs_3Sb_4F_{15}$ ($\sigma = 1.8 \times 10^{-3}$ S/cm, $T \approx 450$ K, Fig. 5, curve 2) can be related as to peculiarities of the structure of these compounds (the structure of $K_3Sb_4F_{15}$ is unknown) as to participation of lighter (in comparison to $Cs^+$ and $Rb^+$) $K^+$ ions in the ionic transport. It is worth mentioning that the diffusion of $F^-$ ions becomes a predominant process in $K_3Sb_4F_{15}$ after the phase transition at 445 K that results in formation of a stable (at least within 2 days) high-temperature β-phase with disordered crystal lattice, in which the fluorine atoms diffusion is preserved until the sample cooling down to 275 K [10,19]. Fluorine atoms participate in the ionic transport; therefore, cooling of β-$K_3Sb_4F_{15}$ results in higher observed ionic conductivity in the sample than at first heating of $K_3Sb_4F_{15}$: this level of conductivity is preserved during repeated heating – β-phase cooling cycles (Fig. 5, curve 2).

## 3. Experimental

### 3.1. Synthesis

Antimony trifluoride, cesium fluoride, and rubidium carbonate of chemical pure grades served as initial substances in synthesis by the preparative method. The $Cs_3Sb_4F_{15}$ compound was obtained at the ratio CsF:$SbF_3$ = 0.9:1, whereas for the synthesis of $CsRb_2Sb_4F_{15}$ the RbF: CsF: $SbF_3$ components ratio was 0.5:0.5:1. Antimony and cesium fluorides samples were dissolved in individual platinum cups upon heating on a water bath. A sample of rubidium carbonate taken in accordance with the equation ($Rb_2CO_3 + 2HF = 2RbF + H_2CO_3$) was added

dropwise with HF until complete dissolution upon heating on a water bath. Thereafter, cesium and rubidium fluorides solutions were mixed; the obtained solution was added with $SbF_3$ solution at stirring and underwent slow crystallization in air. The formed crystalline substances were separated from the solution by vacuum filtration and washed with acetone. The composition of the obtained solid phases was determined by means of the methods of chemical, X-ray diffraction (XRD), and IR spectroscopy analysis according to standard techniques. The Sb calculated content (%) for $Cs_3Sb_4F_{15}$ was 41.60; the found one was 41.6. For $CsRb_2Sb_4F_{15}$, the calculated value was 45.27; the found one was 45.2.

### 3.2. IR spectroscopy

The samples IR absorption spectra were recorded in the range 400–4000 $cm^{-1}$ using a Shimadzu FTIR Prestige-21 Fourier spectrometer (Japan) at room temperature. The measured samples were ground in an agate mortar until finely dispersed state and mixed with Vaseline oil until the formation of a suspension, which was deposited on the KBr substrate.

### 3.3. X-ray study

For X-ray studies, a single crystal of the compound **I** was glued (100% Stronger, No. 401) to a glass needle. The crystal data were recorded at 296 K on a SMART APEX II diffractometer (Mo$K\alpha$-radiation, graphite monochromator, ω-scanning with 0.3° increment in the area of hemisphere of the reciprocal space, the exposure time 20 s per frame at a distance between crystal and detector of 45 mm). Data recording and editing and unit cell refining were performed using the Apex II program package [31]. All the calculations on the structure determination and refining were made using SHELXTL/PC programs [32].

The structure was determined using a direct method and refined on $F^2$ using a full-matrix least-squares method in the anisotropic approximation. Main crystallographic data, experimental parameters, and refinement details are shown in Table 1.

The CIF-file containing full information on the studied structure is deposited to the inorganic compounds structure database ICSD under the number 429644, where it can be obtained free of charge upon request: http://www.ccdc.cam.ac.uk/data_request/cif.

**Table 1**
Crystal data and, experimental and refinement details for the compound **I**.

| Empirical formula | $CsRb_2Sb_4F_{15}$ |
|---|---|
| Formula weight | 1075.85 |
| Temperature (K) | 296(2) |
| Wavelength (Å) | Mo$K_\alpha$ (0.71073) |
| Crystal system | Monoclinic |
| Space group | P2(1)/c |
| *a*, *b*, *c* (Å) | 7.9863(3), 28.5936(11), 8.0319(3) |
| $\alpha$, $\beta$, $\gamma$ (°) | 90, 116.601(1), 90 |
| *V* (Å$^3$) | 1640.0(1) |
| *Z* | 4 |
| Density (calculated) (Mg/м$^3$) | 4.357 |
| Absorption coefficient ($mm^{-1}$) | 14.740 |
| *F*(000) | 1872 |
| Crystal size (mm) | 0.25 × 0.25 × 0.18 |
| $\theta$ range for data collection | 2.85–33.11 |
| Reflections collected | 28676 |
| Independent reflections | 5962 [*R*(int) = 0.0234] |
| Data/restraints/parameters | 5962/0/200 |
| Goodness-of-fit on $F^2$ | 1.081 |
| Final *R* indices [$I > 2\sigma(I)$] | 0.0334 |
| *R* indices (all data) | 0.0377 |
| $\Delta\rho_{max}$, $\Delta\rho_{min}$ (e Å$^{-3}$) | 3.566, −1.627 |

### 3.4. NMR study

The $^{19}F$ NMR spectra of the polycrystalline samples were recorded on a Bruker AVANCE-300 spectrometer at Larmor frequencies $\nu_L$ = 282.404 MHz and temperatures from 150 to 450 K. One-pulse sequence with 2 μs pulse width was used, the relaxation delay was 5 s, and the sampling frequency corresponding to the spectral width was from 1 to 5 MHz. The temperature adjustment accuracy was ±2 K. Calculations of the RMS width of NMR spectra (or the second moment $S_2$, in $G^2$) were performed using an original code by formulas given in [33,34]. The full width at half-maximum of an integral line $\Delta H_{1/2}$ (in kHz) and the chemical shift (CS) (in ppm vs. $C_6F_6$) were estimated from the spectra with an accuracy of 2–4%. Chemical shifts of $C_6F_6$ are −589 ppm relatively to gaseous $F_2$ ($\delta(F_2)$ = 0 ppm) and −167 ppm relatively to $CFCl_3$ [33]. Simulations of experimental $^{19}F$ NMR spectra were carried out by the original computer program, which enables one to perform the spectrum decomposition into components and determine their positions, integrated intensity (in % to the total spectrum area), width, the second moment, and the type of the function describing the shape of the resonance line (Gauss, Lorentz, and etc.). The program fitting of the experimental spectrum was performed by minimization of the sum of squared deviations between experimental and calculated spectral points. The modified Newton's method was used for the minimization. The spectrum simulation accuracy was from 2 to 5%.

### 3.5. Thermal measurements

The thermal properties of fluoroantimonates(III) were studied by Differential Scanning Calorimetry (DSC) (DSC-204F1, NETZSCH, Germany) in a dry argon atmosphere at a heating rate of 10°/min; the error of temperature measurement was 0.2 K

### 3.6. Conductivity measurements

Electrophysical characteristics of the polycrystalline samples under study compressed into tablets of a diameter of 13 mm were determined by the method of impedance spectroscopy. Two surfaces of the samples were covered with Ag paint electrodes and ac-conductivity was measured in vacuum of ~$3 \times 10^{-2}$ Torr within the temperature range of 300–450 K by HP-4284A Precision LCR Meter over the frequency range of 20 to 1 MHz. Conductivity values were estimated from those of real and imaginary parts of complex impedance by the complex impedance technique.

## 4. Conclusions

During the isomorphic substitution of cesium ions by rubidium ions in the compound $Cs_3Sb_4F_{15}$, an isostructural compound $CsRb_2Sb_4F_{15}$ has been obtained. The compound structure is of an isle-like character (monoclinic syngony, space group $P2_1/c$) and built from trigonal $SbEF_4$ bipyramids, two of which are linked into the $[Sb_2F_7]^-$ dimer, whereas the other two remain isolated. Cesium and rubidium atoms link anionic complexes of antimony(III) into a framework. The character of ionic motions in the fluoride sublattice of these compounds upon temperature variation has been investigated. It has been established that the type of ionic mobility in the fluoride sublattice in the temperature range 150–450 K changes according to the following scheme: rigid lattice (below 200 K) → local motions (210–400 K) → anisotropic diffusion (above 420 K). The comparison of conductivities in the compounds $K_3Sb_4F_{15}$, $Cs_3Sb_4F_{15}$, and $CsRb_2Sb_4F_{15}$ has been performed. The lower electroconductivity value in the compound with a heteroatomic cationic sublattice as compared to that of the isostructural compound $Cs_3Sb_4F_{15}$ is, most probably, caused by the

decrease of the number of $Cs^+$ cations with high polarizability in its composition. The specific polarizability in the compound $CsRb_2Sb_4F_{15}$ attains the value of $5.8 \times 10^{-5}$ S/cm at 450 K, which allows its assignment to the class of compounds with high ionic conductivity.

## Acknowledgment

The authors are grateful to the Russian Foundation for Basic Research (project no. 14-03-00041) for partial financial support.

## Appendix A. Supplementary data

Supplementary data associated with this article can be found, in the online version, at http://dx.doi.org/10.1016/j.jfluchem.2015.07.014.

## References

[1] A.A. Udovenko, L.M. Volkova, Sov. J. Coord. Chem. 7 (1981) 1763–1813.
[2] L.A. Zemnukhova, R.L. Davidovich, Z. Naturforsch. 53a (1998) 573–584.
[3] M.P. Borzenkova, F.V. Kalinchenko, A.V. Novoselova, A.K. Ivanov-Schits, N.I. Sorokin, Russ. J. Inorg. Chem. 29 (1984) 703–705 (Engl. Transl.).
[4] R.L. Davidovich, P.S. Gordienko, J. Grigas, T.A. Kaidalova, V. Urbonaviciu, L.A. Zemnukhova, Phys. Status Solidi (a) 84 (1984) 387–392.
[5] V.N. Serezhkin, Y.A. Buslaev, Zh. Neorg. Khim. 42 (1997) 1180–1187 (in Russian).
[6] V.I. Sergienko, V.Y. Kavun, L.N. Ignateva, Zh. Neorg. Khim. 36 (1991) 3153–3158 (in Russian).
[7] V.Y. Kavun, V.I. Sergienko, Diffusive Mobility and Ionic Transport in Crystal and Amorphous Fluorides of IV Groups Elements and Antimony(III), Dalnauka, Vladivostok, 2004p. 298 (in Russian).
[8] L.A. Zemnukhova, G.A. Fedorishcheva, Russ. Chem. Bull. 1 (1999) 103–108 (Engl. Transl.).
[9] N.V. Makarenko, A.A. Udovenko, L.A. Zemnukhova, V.Y. Kavun, M.M. Polyantsev, J. Fluor. Chem. 168 (2014) 184–188.
[10] V.Y. Kavun, N.F. Uvarov, A.B. Slobodyuk, O.V. Brovkina, L.A. Zemnukhova, V.I. Sergienko, Russ. J. Electrochem. 41 (2005) 488–500 (Engl. Transl.).
[11] V.Y. Kavun, M.M. Polyantsev, L.A. Zemnukhova, A.B. Slobodyuk, V.I. Sergienko, J. Fluor. Chem. 168 (2014) 198–203.
[12] K. Yamada, Y. Ohnuki, H. Ohki, T. Okuda, Chem. Lett. 7 (1999) 627–628.
[13] B. Ducourant, R. Fourcade, C. R. Acad. Sci. 282C (1976) 741–744, Paris.
[14] V.Y. Kavun, A.A. Udovenko, N.F. Uvarov, V.I. Sergienko, L.A. Zemnukhova, J. Struct. Chem 43 (2002) 246–251.
[15] A.A. Udovenko, Y.E. Gorbunova, L.A. Zemnukhova, et al. Russ. J. Coord. Chem. 27 (2001) 479–482.
[16] L.N. Ignateva, V.I. Sergienko, V.Y. Kavun, T.F. Antokhina, I.A. Sil'chenko, Zh. Neorg. Khim. 35 (1990) 1532–1536 (in Russian).
[17] L.A. Zemnukhova, A.A. Udovenko, N.V. Makarenko, G.A. Fedorishcheva, V.Y. Kavun, A.B. Slobodyuk, N.A. Didenko, J. Fluor. Chem. 156 (2013) 298–302.
[18] A.G. Lundin, E.I. Fedin, NMR Spectroscopy, Nauka, Moscow, 1986.
[19] N.F. Uvarov, V.Y. Kavun, L.A. Zemnukhova, Proceedings of the First International Siberian Workshop "Advances Inorganic Fluorides", Novosibirsk, Russia, 2003, 236–242.
[20] V.Y. Kavun, N.F. Uvarov, V.I. Sergienko, L.A. Zemnukhova, Russ. J. Coord. Chem. 30 (2004) 505–510 (Engl. Transl.).
[21] Y.N. Moskvich, B.I. Cherkasov, M.A. Polyakov, et al. Phys. Status Solidi (b) 156 (1989) 615–631.
[22] V.Y. Kavun, L.A. Zemnukhova, V.I. Sergienko, T.A. Kaidalova, R.L. Davidovich, N.I. Sorokin, Russ. Chem. Bull. Int. Ed. 51 (2002) 1996–2002.
[23] V.Y. Kavun, N.F. Uvarov, L.A. Zemnukhova, A.S. Ulikhin, N.A. Didenko, O.V. Brovkina, V.I. Sergienko, Russ. J. Electrochem. 49 (2013) 633–644 (Engl. Transl.).
[24] V.Y. Kavun, A.V. Gerasimenko, V.I. Sergienko, R.L. Davidovich, N.I. Sorokin, Russ. J. Appl. Chem. 73 (2000) 1025–1029 (Engl. Transl.).
[25] V.Y. Kavun, V.I. Sergienko, N.F. Uvarov, T.F. Antokhina, J. Struct. Chem. 43 (2002) 429–435.
[26] V.Y. Kavun, S.P. Gabuda, S.P. Kozlova, R.L. Davidovich, J. Struct. Chem. 40 (1999) 541–547.
[27] J.M. Réau, J. Portier, A. Levasseur, G. Villeneuve, M. Pouchard, Mater. Res. Bull. 13 (1978) 1415–1423.
[28] R.C. Agrawal, R.K. Gurta, J. Mater. Sci. 34 (1999) 1131–1162.
[29] V. Trnovcová, P.P. Fedorov, I. Furar, Russ. J. Electrochem. 45 (2009) 630–639.
[30] R.D. Shannon, R.X. Fischer, Phys. Rev. B 73 (2006) 235111–235128.
[31] Bruker, APEX2, Bruker AXS Inc., Madison, Wisconsin, USA, 2005.
[32] G.M. Sheldrick, Acta Crystallogr. Sect. A 64 (2008) 112–122.
[33] S.P. Gabuda, Y.V. Gagarinskiy, S.A. Polishchuk, NMR in the Inorganic Fluorides, Atomizdat, Moscow, Russia, 1978.
[34] C.P. Slichter, Principles of Magnetic Resonance, 3rd Enl. Upd. Ed., Springer-Verlag, Berlin, 1992.